REPORT DOCUMENTATION PAGE

Form Approved
OMB No. 0704-0188

1. REPORT DATE *(DD-MM-YYYY)*	**2. REPORT TYPE**	**3. DATES COVERED** *(From - To)*
September 2013	Journal Article	September 2013- October 2013

4. TITLE AND SUBTITLE
Helium Nanodroplet Isolation and Infrared Spectroscopy of the Isolated Ion-Pair 1-ethyl-3-methylimidazolium bis(trifluoromethylsulfonyl)imide

5a. CONTRACT NUMBER
In-House

5b. GRANT NUMBER

5c. PROGRAM ELEMENT NUMBER

6. AUTHOR(S)
E.I. Obi, C.M. Leavitt, P.L.Raston, C.P. Moradi, S.D Flynn, J.A. Boatz, S.D. Chambreau, G.E. Douberly

5d. PROJECT NUMBER

5e. TASK NUMBER

5f. WORK UNIT NUMBER
Q0RA

7. PERFORMING ORGANIZATION NAME(S) AND ADDRESS(ES)

Air Force Research Laboratory (AFMC)
AFRL/RQRP
10 E. Saturn Blvd.
Edwards AFB CA 93524-7680

8. PERFORMING ORGANIZATION REPORT NO.

9. SPONSORING / MONITORING AGENCY NAME(S) AND ADDRESS(ES)
Air Force Research Laboratory (AFMC)
AFRL/RQR
5 Pollux Drive
Edwards AFB CA 93524-7048

10. SPONSOR/MONITOR'S ACRONYM(S)

11. SPONSOR/MONITOR'S REPORT NUMBER(S)
AFRL-RQ-ED-JA-2013-208

12. DISTRIBUTION / AVAILABILITY STATEMENT
Distribution A: Approved for Public Release; Distribution Unlimited. PA#13471

13. SUPPLEMENTARY NOTES
Journal Article submitted to Journal of Physical Chemistry.

14. ABSTRACT
The ionic liquid 1-ethyl-3-methylimidazolium bis(trifluoromethylsulfonyl)imide is vaporized at 420 K, and the ion-pair constituents are entrained in a beam of liquid He nanodroplets and cooled to 0.4 K. The vapor pressure is optimized such that each He droplet picks up a single ion-pair from the gas phase. Infrared spectroscopy in the CH stretch region reveals bands that are assigned to intact ion-pairs on the basis of comparisons to *ab initio* harmonic frequency computations of 23 low energy isomers. The He droplet spectrum is consistent with a weighted sum of the computed harmonic spectra, in which the weights are determined from *ab initio* computations of the relative free energies at 420 K. Anharmonic resonance polyads in the CH stretch region are treated explicitly, which improves the agreement between the experiment and computed spectra for ion-pairs. For isomers having a strong cation…anion hydrogen bonding interaction, the imidazolium C(2)-H stretch fundamental is shifted to lower energy and into resonance with the overtones and combination of the imidazolium ring stretching modes, resulting in a spectral complexity in the CH stretch region that is fully resolved in the He droplet spectrum. The assignment of the infrared spectrum to ion-pairs is confirmed through polarization spectroscopy measurements that reveal the permanent electric dipole moment of the He-solvated species to be 11□2 D. The computed permanent electric dipole moments for the low energy isomers of the [emim+][Tf2N-] ion pairs fall in the range 9-13 D, whereas the computed dipole moments of decomposition products of the ionic liquid are less than 4.3 D.

15. SUBJECT TERMS

16. SECURITY CLASSIFICATION OF:			**17. LIMITATION OF ABSTRACT**	**18. NUMBER OF PAGES**	**19a. NAME OF RESPONSIBLE PERSON**
					Tom Hawkins
a. REPORT	**b. ABSTRACT**	**c. THIS PAGE**			**19b. TELEPHONE NO** *(include area code)*
Unclassified	**Unclassified**	**Unclassified**	SAR	31	661-525-5449

Standard Form 298 (Rev. 8-98)
Prescribed by ANSI Std. 239.18

Helium Nanodroplet Isolation and Infrared Spectroscopy of the Isolated Ion-Pair 1-ethyl-3-methylimidazolium bis(trifluoromethylsulfonyl)imide

Emmanuel I. Obi[†], Christopher M. Leavitt[†], Paul L. Raston[†], Christopher P. Moradi[†], Steven D. Flynn[†], Jerry A. Boatz[§,*], Steven D. Chambreau[‡,*] and Gary E. Douberly[†,*]

[†]Department of Chemistry, University of Georgia, Athens, GA 30602

[§]Air Force Research Laboratory, Edwards Air Force Base, CA 93524

[‡]ERC Incorporated, Edwards Air Force Base, CA 93524

Corresponding authors: jerry.boatz@us.af.mil [§,*] steven.chambreau.ctr@us.af.mil [‡,*]

douberly@uga.edu [†,*]

Abstract

The ionic liquid 1-ethyl-3-methylimidazolium bis(trifluoromethylsulfonyl)imide is vaporized at 420 K, and the ion-pair constituents are entrained in a beam of liquid He nanodroplets and cooled to 0.4 K. The vapor pressure is optimized such that each He droplet picks up a single ion-pair from the gas phase. Infrared spectroscopy in the CH stretch region reveals bands that are assigned to intact ion-pairs on the basis of comparisons to *ab initio* harmonic frequency computations of 23 low energy isomers. The He droplet spectrum is consistent with a weighted sum of the computed harmonic spectra, in which the weights are determined from *ab initio* computations of the relative free energies at 420 K. Anharmonic resonance polyads in the CH stretch region are treated explicitly, which improves the agreement between the experiment and computed spectra for ion-pairs. For isomers having a strong cation···anion hydrogen bonding interaction, the imidazolium $C_{(2)}$-H stretch fundamental is shifted to lower energy and into resonance with the overtones and combination of the imidazolium ring stretching modes, resulting in a spectral complexity in the CH stretch region that is fully resolved in the He droplet spectrum. The assignment of the infrared spectrum to ion-pairs is confirmed through polarization spectroscopy measurements that reveal the permanent electric dipole moment of the He-solvated species to be 11±2 D. The computed permanent electric dipole moments for the low energy isomers of the [$emim^+$][Tf_2N^-] ion-pairs fall in the range 9-13 D, whereas the computed dipole moments of decomposition products of the ionic liquid are less than 4.3 D.

Introduction

Ionic liquids are low melting point salts (< 373 K) whose bulky constituents lead to characteristically long cation-anion distances and low lattice energies, in comparison to common ionic salts, such as NaCl.[1, 2] For many cation-anion combinations, ionic liquids possess properties such as low volatility, thermal stability, and a marked stability towards air and water. In principle, these physical and chemical properties can be tuned by the choice of cation-anion combination, making ionic liquids potentially useful for batteries,[3-5] solar cells,[6, 7] fuel cells,[8, 9] and as "green" solvents[10] for organic synthesis and chromatography.[11] Ionic liquids have also been shown to exhibit considerable promise as fuels for electrospray ion thrusters in space propulsion applications.[12-14] Chambreau and co-workers reported a class of room temperature ionic liquids (RTILs) that spontaneously ignite upon the introduction of a strong oxidizer, such as fuming nitric acid,[15, 16] and other groups have more recently reported the ignition of RTILs with nitric acid,[17-19] nitrogen tetroxide,[20] and hydrogen peroxide.[21] This observed hypergolic activity suggests that a properly chosen RTIL / oxidizer combination could replace the highly volatile and environmentally toxic hydrazine-based hypergolic fuels currently used in bipropellant rocket engines.[16] Given the vast number of cation-anion combinations, it is impractical to experimentally characterize even a small fraction of all possible RTILs. The optimization of these systems for use in the above applications will therefore require predictive models of RTIL properties. The molecular level understanding on which these models must be based will be partially derived from experimental methods capable of probing the fundamental aspects of RTILs isolated *in vacuo*, such as high resolution spectroscopy. We report here the vibrational spectrum and dipole moment of a prototype RTIL that is vaporized and entrained in a beam of liquid He nanodroplets.

Until recently, it was presumed that RTILs possess essentially no vapor pressure, due to the ionic nature of the liquid. Earle and co-workers were the first to demonstrate, however, that the vacuum distillation of certain families of aprotic RTILs could be achieved below the decomposition temperature of the material.[22] This result pointed towards the possibility of gas-phase experiments, and many reports have since been presented that investigate both the nature of the ionic liquid vapor and the vaporization mechanism. For many of these gas phase studies,

the ionic liquid [1-ethyl-3-methylimidazolium][bis(trifluoromethylsulfonyl)imide] (abbreviated [$emim^+$][Tf_2N^-]; see Scheme 1 and Figure 1) was used due to its low viscosity and high thermal stability at the temperatures required to produce a sufficient vapor pressure. This prototypical RTIL has been studied *in vacuo* with line of sight electron impact mass spectrometry (MS),[23] VUV photoionization MS,[24, 25] FTICR-MS,[26] selected-ion flow tube MS.[27] These indirect probes of the neutral gas-phase constituents are all consistent with the vaporization of individual ion-pairs with little or no decomposition. Consistent with this, enthalpies of vaporization (ΔH_{vap}) were computed to be lowest for ion-pairs[28], and computations of ΔH_{vap} [29] for [$emim^+$][Tf_2N^-] agree well with experiment.[30] Furthermore, the valence binding energy spectrum obtained from photoelectron spectroscopy[29] and the photoionization appearance energy measured with tunable VUV synchrotron radiation[31] are in agreement with computed valence binding energies and adiabatic ionization potentials of individual ion-pairs. Collectively, these studies of vaporized 1-alkyl-3-methylimidizolium based ionic liquids provide strong evidence for intact ion-pairs.[32] Two studies have directly detected the intact ion-pairs of a similar dialkylimidazolium-based RTIL.[33, 34] Nevertheless, there has been a lack of experimental studies capable of probing the detailed geometric structure of these gas-phase, isolated ion-pairs.

SCHEME 1

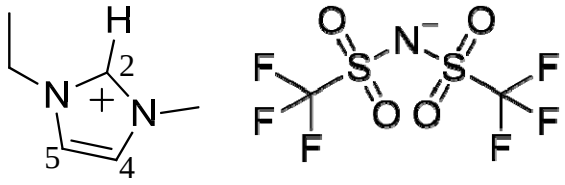

There is a growing literature of *ab initio* and DFT computations of the geometric structure and electronic properties of gas-phase, ionic liquid ion-pairs.[35-43] Computations predict several conformational isomers associated with isolated [$emim^+$][Tf_2N^-] ion-pairs,[42, 44] and even for this highly studied system, there still remains significant debate over the preferred geometric structure. There is generally little agreement on the relative role of charge-charge, hydrogen bonding and pi-stacking interactions in determining the structure of isolated ion-pairs.[45] Tsuzuki and co-workers have downplayed the importance of the orientation of the [Tf_2N^-] anion relative to the acidic imidazolium $C_{(2)}H$ bond and suggested instead that the dominant charge-charge interactions result in a rather flat potential surface with many isomers having similar binding energies.[42] On the other hand, hydrogen bonded structures with multiple C-H···X hydrogen

bonds (X = N, F, or O) are often invoked in order to assign vibrational bands in condensed phase IR spectroscopy experiments of [emim$^+$][Tf_2N^-].[46-50] For example, in cryogenic neon matrix isolation experiments,[44, 51, 52] it was concluded that [emim$^+$][Tf_2N^-] structures having strong in plane $C_{(2)}H^{+\cdots}N^-$ hydrogen bonds were present in large abundance on the basis of comparisons between the experimental FTIR spectra in the 52 to 1700 cm^{-1} region and *ab initio* harmonic frequency computations.[44]

The analysis of many of these condensed phase studies (liquid room temperature or cryogenic matrix isolation) have relied only on comparisons between FTIR spectra and DFT or *ab initio* (MP2 level of theory) harmonic frequency computations. Interestingly, a recent computation of the cubic force constants for the bare [emim$^+$] cation suggests the presence of strong anharmonic resonances in the CH stretch region.[53] This motivated Lassègues and co-workers to reassign the CH stretch region of condensed phase FTIR spectra to a class of structures that does not involve strong, directional $C_{(2)}H^{\cdots}$anion hydrogen bonds.[53, 54] The conclusions drawn by these authors from these anharmonic frequency computations contradict those of several previous reports that relied on the relative intensities of bands in the CH stretch region to make inferences about the structural properties of the liquid.[46] Given this disagreement[55, 56] that persists in the literature, there is a clear need for high resolution IR spectroscopic methods that probe the structure of isolated gas phase ion-pairs. Helium Nanodroplet Isolation is a well suited method for this purpose.[57-62] The large capture cross sections associated with He droplets allows for the pick-up, trapping, cooling, and spectroscopic interrogation of fragile species that have relatively low vapor pressures. Over a 1 cm path length, only $\approx 10^{11}$ molecules/cm^3 (10^{-5} Torr) are required to dope the droplets with single RTIL constituent molecules. The weakly perturbing He solvent allows for highly resolved vibrational spectroscopy studies of the solvated molecular species, which can be compared directly to the predictions of quantum chemistry. Indeed, when comparisons are available, the vibrational band origins of He-solvated molecules and molecular complexes differ little from those measured in the gas phase (~1 cm^{-1} or less).[57]

As discussed in the present report, the prototypical RTIL, [emim$^+$][Tf_2N^-], was vaporized at 410 K and entrained in liquid He droplets. On the basis of previous reports employing this methodology,[63, 64] we expect the gas phase thermal distribution of [emim$^+$][Tf_2N^-] isomers to be

"frozen-out" due to the rapid dissipation of the molecular internal energy upon He solvation. The IR spectrum in the CH stretch region is consistent with a 420 K thermal distribution of intact ion-pairs, having *both* hydrogen bonded and stacked structures. The high resolution associated with this measurement allows for a direct comparison of the observed spectrum to *ab initio* frequency computations of 23 [emim$^+$][Tf_2N^-] isomers. For satisfactory agreement between experiment and theory, the anharmonic coupling between ring stretching overtones and CH stretching fundamentals must be explicitly considered, indicating that strong anharmonic resonances persist in this spectral region, as originally suggested by Lassègues and co-workers.[53] Furthermore, the intensity of a well-resolved IR band was measured as the He-solvated molecule was oriented in a lab-frame electric field. This polarization spectroscopy measurement is consistent with an [emim$^+$][Tf_2N^-] permanent electric dipole moment of 11±2 D, which corroborates the assignment of its structure to an isolated ion-pair.

Experimental Methods

Helium droplets are formed (10^{12} s^{-1}) by the continuous expansion of He gas (30 bar) through a 5 μm diameter pin-hole nozzle. The nozzle is cooled by a closed-cycle refrigerator to ≈14 K. The average droplet size under these source conditions is ≈6000 He atoms.[65, 66] Upon leaving the high pressure region of the expansion, the droplets cool by evaporation to 0.4 K.[67, 68] The droplet expansion is skimmed into a beam, which then passes into a differentially pumped "pick-up" chamber. The droplets are doped with [emim$^+$][Tf_2N^-] as the beam passes directly above the opening to a resistively heated quartz oven containing the liquid. Zaitsau, *et. al*. used the integral effusion Knudsen method to obtain [emim$^+$][Tf_2N^-] vapor pressures.[30] Extrapolating their data, we find that an oven temperature of 440 K produces the ≈1.5 x 10^{-5} Torr vapor pressure required for each droplet to pick-up one [emim$^+$][Tf_2N^-] ion-pair, on average. The IR spectra are measured with the oven source at 420 K to reduce the vapor pressure slightly below what is optimal for the pick-up of a single ion-pair. Under these conditions, the probability of sequentially picking up two ion-pairs into the same droplet is less than 10% that of picking up one, and the consideration of the cluster spectra can be neglected. Previous photoionization mass spectrometry [24] and photoelectron spectroscopy [29] studies of [emim$^+$][Tf_2N^-] used an effusive

oven source at ≈470 K, and no evidence of decomposition was found. The internal energy of He-solvated [$emim^+$][Tf_2N^-] is removed by He atom evaporation and the system returns to 0.4 K within a nanosecond of pick-up.[69] During this process, each evaporating He atom removes on average 5 cm^{-1} (0.014 kcal/mol) of energy.[69] Due to this rapid cooling of the He droplet upon ion-pair pick-up, the distribution of conformational isomers in the droplets is expected to resemble the equilibrium distribution in the vapor, as has been observed for other multi-isomeric systems.[57, 63, 64]

The He droplets are detected with a quadrupole mass spectrometer equipped with an electron impact ionizer (90 eV), which provides signatures of both the neat and doped fractions of the droplet ensemble. To optimize for the pick-up of single ion-pairs, the oven temperature is adjusted while monitoring the mass spectrum of the droplet beam, as described below. The IR spectrum of the He-solvated [$emim^+$][Tf_2N^-] ion-pair is obtained by overlapping the droplet beam with the output from a continuous wave IR Optical Parametric Oscillator (OPO) laser system.[70] This overlap is achieved by either counter-propagating the OPO and droplet beams or by steering the OPO beam into a multipass cell, consisting of two parallel gold-coated mirrors. Vibrational excitation of the solvated [$emim^+$][Tf_2N^-] ion-pair followed by vibrational relaxation results in the evaporation of ≈620 He atoms for CH stretch excitation near 3100 cm^{-1}. This geometric cross-section reduction leads to a concomitant decrease in the electron impact ionization cross-section of the [$emim^+$][Tf_2N^-] doped He droplets as they enter into the mass spectrometer. The [$emim^+$][Tf_2N^-] IR spectrum is obtained by monitoring the depletion of the ion signal (normalized to laser power) as the OPO counter-propagates the droplet beam and is tuned from 2800-3300 cm^{-1}. The dipole moment measurements described below are obtained with the OPO aligned into the multipass cell. In this configuration, the entire droplet beam / laser interaction region is contained within a static dc electric field established between two parallel stainless steel electrodes situated orthogonal to the multipass mirrors. The laser polarization is aligned parallel to this static electric field with a Fresnel Rhomb. The OPO wavelength is fixed to the peak of an IR transition, and the electric field is linearly ramped from 0-30 kV/cm. The field ON to field OFF intensity ratio of the IR band is averaged for about 10 of these scans.

Theoretical Methods

Previously, Tsuzuki and co-workers found that the *ab initio* (MP2/6-311G**) interaction energy between cation and anion in [emim$^+$][Tf_2N^-] is somewhat insensitive to their relative orientations, and they found 16 conformational isomers with electronic energies within 10 kJ/mol of the lowest energy species.[42, 43] We have carried out geometry optimizations and harmonic frequency computations at the MP2/aug-cc-pVTZ level[71-75] of theory using GAMESS[76, 77] for 23 low energy isomers, starting from the structures reported in Ref. [42]. Here, the harmonic frequencies are scaled by 0.96, and these scaled values are used to determine zero-point vibrational energies and thermal corrections. The five lowest energy [emim$^+$][Tf_2N^-] ion-pair isomers at this level are shown in Fig. 1 and numbered **1-5** according to their relative zero-point corrected electronic energies. The relative Gibbs free energies computed at 420 K are 0.70, 1.37, 0.00, 3.81 and 5.91 kJ/mol for isomers **1-5**, respectively. The entropic effect is to make isomer **3** the most abundant configuration at thermal equilibrium. However, we emphasize that the relative free energies of these five isomers are within the error bars of the calculation ($\pm \approx 5$ kJ/mol), and it is therefore difficult to know with any certainty, at this level of theory, which isomer is actually the most stable one. The structures for the complete set of 23 isomers along with their relative energetics and computed spectra are given in the Supporting Information.

The vibrational transition moment angles (VTMAs)[63, 78] and permanent electric dipole moment vectors (μ_p) are computed at this same level of theory for each [emim$^+$][Tf_2N^-] isomer. For any one normal mode vibration, the VTMA is defined as the angle μ_p makes with the transition dipole moment vector (μ_t). Orientation of the He-solvated molecules in a static electric field allows for the simultaneous measurement of μ_p and the VTMA associated with a particular band in the IR spectrum.[78, 79] This is achieved by measuring the field dependence of the IR band intensity. By choosing a combination of VTMA and μ_p, this field dependence of the IR intensity can be simulated and compared to the experiment. In the simulation, the average projection of μ_t onto the OPO polarization axis is determined for field strengths in the range 0-30 kV/cm. The weighting function for this average is the normalized orientational distribution of μ_p about the lab-frame static field axis. This dipole distribution function, $P(\cos\theta)$, is computed for each static electric field strength (increments of 5 kV/cm) according to the procedures of Kong and

Bulthuis.[80, 81] Here, θ is defined as the angle between μ_p and the static field axis. Calculations of $P(\cos\theta)$ are based on the *ab initio* rotational constants (divided by 3 to account for the helium solvent)[57] and inertial dipole moment components for isomer **3** and a rotational temperature of 0.4 K. While the computed orientational distribution is sensitive to the magnitude of μ_p, a quantitative determination of rotational constants is not required for a relatively "heavy" system, such as $[emim^+][Tf_2N^-]$. Indeed, the simulation will be insensitive to the exact values of the rotational constants, given that the interaction between the dipole moment and the electric field is much larger than the average $[emim^+][Tf_2N^-]$ rotational energy at 0.4 K. With the computed $P(\cos\theta)$ distribution, μ_t is projected onto the polarization axis of the OPO (parallel to the lab-frame field axis) and averaged over θ to give the relative intensity, A_{para}, due to molecular orientation at a given field strength,[82] where α is the VTMA:

$$A_{para}(\alpha) \propto \int_{-1}^{1} P(\cos\theta)[\sin^2\alpha + 2\cos^2\theta - 3\sin^2\alpha\cos^2\theta]d\cos\theta\,. \qquad (1)$$

Results and Discussion

A. Mass Spectrometry

Electron impact ionization of a He droplet produces a solvated He^+ cation, which leads to a vibrationally excited He_2^+ cation. The outcome of this ionization process is now well known to produce a distribution of gas phase He_n^+ ions.[83] The mass spectrum in Fig. 2a shows the He_n^+ ions associated with the ionization of the neat droplet beam. If the droplets are doped, in addition to the He_n^+ distribution, ions associated with the solvated molecule can be produced as a result of the charge transfer reaction,

$$He^+ + \text{dopant} \rightarrow He + [\text{dopant}]^+ \rightarrow He + [\text{dopant fragments}]^+. \qquad (2)$$

Figures 2b-d show the evolution of the mass spectrum as the quartz oven source is heated to dope the droplets with $[emim^+][Tf_2N^-]$. Due to the ionization of what is presumably the He-solvated $[emim^+][Tf_2N^-]$ ion-pair, heating the oven to 408 K results in a new peak in the mass

spectrum at m/z=111. This peak corresponds to the non-fragmented [$emim^+$] cation. Upon heating the oven further to 426 K, the peak at m/z=111 becomes more intense and other peaks in the lower mass range begin to appear. The neat He droplet mass spectrum (Fig. 2a) is subtracted from the mass spectrum recorded with the oven at 426 K (Fig. 2d), giving the difference spectrum shown in Fig. 3. With the He peaks subtracted, the remaining peaks are due only to ions formed upon He^+ charge transfer to species picked-up by the droplet beam. In addition to m/z=111, other predominant peaks in the mass spectrum such as m/z=31, 50, 64, 69 are due to CF^+, CF_2^+, SO_2^+, and CF_3^+, respectively, which are fragments from [Tf_2N^-]. In previous line of sight electron impact ionization mass spectrometry [23] and VUV soft photoionization studies,[24] the dominance of the m/z=111 [$emim^+$] peak was interpreted as being due to the dissociative ionization of [$emim^+$][Tf_2N^-] ion-pairs in the gas phase, according to the mechanism

$$[emim^+]\,[Tf_2N^-] + h\nu \rightarrow [emim^+]\,[Tf_2N] + e^- \rightarrow [emim^+] + [Tf_2N] + e^-. \qquad (3)$$

A similar dissociative ionization mechanism is likely operative upon electron impact ionization of [$emim^+$][Tf_2N^-] doped He droplets. This appears reasonable because the ionization of [$emim^+$][Tf_2N^-] is only likely to proceed via He^+ charge transfer, and the difference in the He and [$emim^+$][Tf_2N^-] ionization potentials is ≈15 eV, which is much larger than the ≈0.5 eV binding energy of the cation-radical complex formed upon ionization. Therefore, the dominance of m/z=111 in the He droplet mass spectrum provides strong evidence for the efficient pick-up of [$emim^+$][Tf_2N^-] ion-pairs.

B. Infrared Spectroscopy

The IR spectrum shown in Figure 4 (middle trace) is obtained by monitoring the ion depletion signal in mass channel m/z=111 as the OPO is continuously tuned from 2800 to 3250 cm^{-1}. There are several spectral features in this wavelength region, presumably due to the CH stretches of [$emim^+$][Tf_2N^-] ion-pairs. The ≈2 cm^{-1} linewidth of each band is broader than the expected rotational contour at 0.4 K, and this width is therefore attributed to the vibrational relaxation timescale of the excited molecule (i.e. ≈3 ps). The red trace at the top of Fig. 4 is the Boltzmann weighted sum of the *ab initio* harmonic spectra (weights determined from free

energies at 420 K). There are three distinctive CH stretching regions of the computed harmonic spectra, and these correspond to the symmetric stretching motions of the imidazolium (IM) alkyl side chains (2950 to 3000 cm^{-1}), the antisymmetric stretching motions of the alkyl side chains (3000 to 3100 cm^{-1}), and the three CH stretches on the IM ring (3090 to 3200 cm^{-1}). The IM ring CH stretch modes consist of the symmetric and antisymmetric stretching motions of the H-$C_{(4)}$-$C_{(5)}$-H group (≈3190 cm^{-1} and ≈3175 cm^{-1}, respectively) and the $C_{(2)}$-H stretch. The computed CH stretches are rather weak, with the majority having intensities less than 15 km/mol. The exceptions to this are the $C_{(2)}$-H stretching bands associated with those isomers that have $C_{(2)}H^{+\cdots}$anion H-bonded configurations (e.g. isomer **3**). For these configurations, the strong, in-plane H-bonds lead to characteristic red shifts and intensity enhancements for the $C_{(2)}$-H stretching bands. The predicted $C_{(2)}$-H band origins range from ≈3090 cm^{-1} for the most strongly H-bonded isomer (isomer **3**) to ≈3160 cm^{-1} for the "non-H-bonded" isomers (isomers **1** and **2**). The $C_{(2)}$-H stretching bands are labeled with bold numbers above the red trace in Fig. 4 to indicate the associated isomer.

Although the weighted *ab initio* spectrum allows for a qualitative assignment of the experiment, there is a degree of spectral complexity in the H-bonded $C_{(2)}$-H stretch region that is not reproduced in the harmonic frequency computations. Indeed, the number of transitions and their relative positions and intensities are not reproduced in the 3050-3150 cm^{-1} region. One possible origin of this discrepancy is the accuracy associated with the relative free energies used to weight the simulated spectrum. It is not obvious *a priori* whether or not the calculations are capable of determining the relative energetics for these lowest five isomers to an accuracy of a few kJ/mol. Another potential source of error is the harmonic approximation employed to compute the vibrational spectrum. Lassègues and co-workers computed (B3LYP/6-31G**) cubic force constants for the bare [$emim^+$] cation and suggested that the relatively large magnitudes for some of these should result in anharmonic resonances in the CH stretch region for IM based RTILs.[53] Indeed, these computations do indicate that the IM CH stretches are coupled to the overtones and combination of two IM ring vibrations near 1600 cm^{-1}, as the cubic force constants associated with these couplings are particularly large (≈70 cm^{-1}) and the energy differences of the modes involved are relatively small. This motivates an analysis of the

observed vibrational complexity in the 3050-3150 cm^{-1} region in terms of anharmonic resonances between the IM ring stretching overtones/combination and the IM CH stretches.

The spectral features associated with these predicted anharmonic resonances can be estimated with a reduced dimensional model that treats the anharmonic couplings explicitly by diagonalizing the 6x6 coupling matrix shown in eq. 4. Here, ν_1 through ν_3 are the fundamental symmetric $C_{(4,5)}$-H, antisymmetric $C_{(4,5)}$-H, and $C_{(2)}$-H stretching modes, respectively; ν_4 and ν_5 are the fundamental antisymmetric and symmetric ring breathing modes, respectively. The diagonal elements are the harmonic frequencies (MP2/aug-cc-pVTZ), which have been scaled by 0.96 to account for diagonal anharmonicity. In this model, the potential expansion is truncated at the cubic terms, and the only non-negligible interactions are those that couple the high frequency CH stretch fundamentals to the overtones/combination of the two lower frequency ring modes. Moreover, any interactions involving the alkyl CH stretch modes are neglected, because these are expected to be only weakly coupled to the vibrations in the ring. The cubic force constants are taken from Ref. [53], and the multiplicative factors in the off-diagonal matrix elements originate from the matrix elements of the normal coordinates in the harmonic oscillator basis.[84, 85] This model further assumes that the cubic force constants do not depend on the presence of the anion, given that they were computed only for the bare [$emim^+$] cation.[53] The intensities of the fundamental CH stretch basis modes are those computed with the harmonic approximation, and the zeroth-order intensities for $2\nu_4$, $2\nu_5$ and $\nu_4+\nu_5$ are set to zero, which is justified given the harmonic nature of the potential energy surface along the ν_4 and ν_5 normal coordinates.[50] For simplicity, we estimate the anharmonic intensities as , in which **i** is the harmonic intensity vector and **U** is a matrix containing the squares of the eigenvector coefficients. This treatment is carried out for isomers **1**-**5**, and the resulting spectra are Boltzmann weighted and summed to give the blue simulation shown at the bottom of Fig 4. In this anharmonic simulation, the transition frequencies and intensities for the alkyl group CH stretches are the same as those in the harmonic simulation. The individual anharmonic spectra for each isomer are given in the Supporting Information.

This simple approximate model leads to a noticeable improvement in the agreement between the experiment and the number of intense bands predicted in the simulation, which again assumes a thermal distribution of ion-pair isomers. The CH stretch transitions above 3150

cm^{-1} are similar to those in the harmonic simulation, with the anharmonic coupling resulting in a 5-10 cm^{-1} blue shift for each of these bands. This relatively modest perturbation of the $C_{(4,5)}$-H stretch vibrations is due to the large energy differences between these modes and the ring overtones/combination. Similarly, the non-H-bonded $C_{(2)}$-H stretches of the "stacked" isomers (**1**, **2** and **5**) are largely unperturbed. One or more these isomers are likely present in the distribution, because the broad feature near 3150 cm^{-1} agrees well with the predicted $C_{(2)}$-H stretch origins for these species. In contrast to these higher frequency modes, significant perturbations are observed for the lower frequency $C_{(2)}$-H stretch modes associated with isomers containing strong, directional $C_{(2)}H^{+\cdots}$anion H-bonds. The H-bonding interaction shifts the $C_{(2)}$-H stretch to lower energy and into resonance with the ring overtones/combination, resulting in significant mode mixing and intensity borrowing. For example, the predicted $C_{(2)}$-H stretch bands for isomers **3** and **4** (scaled harmonic 3093 and 3107 cm^{-1}, respectively) are particularly intense due to H-bonding, and the interaction between these modes and the ring overtone/combination states results in a characteristic four peak pattern for each isomer. This predicted pattern for these H-bonded isomers is consistent with that observed experimentally between 3050 and 3125 cm^{-1}. We emphasize, however, that the band positions and intensities are rather sensitive to both the magnitude of the coupling constants and the zeroth-order band origins, and we therefore do not expect to achieve quantitative agreement between the experiment and simulation at this level of theory and with this approximate model. The arrows and brackets in Fig. 4 indicate the suggested assignments. In general, the agreement between the Boltzmann weighted anharmonic simulation and the experimental IR spectrum suggests that the droplets pick-up and cool a gas-phase distribution of *ion-pair* isomers (both H-bonded and non-H-bonded), which are at thermal equilibrium at the ≈420 K source temperature; otherwise, at 0.4 K, only the lowest free energy isomer would be expected.

$$\begin{vmatrix} \nu_1 & 0 & 0 & \varphi_{144}/4 & \varphi_{155}/4 & \varphi_{145}/8^{1/2} \\ & \nu_2 & 0 & \varphi_{244}/4 & \varphi_{255}/4 & \varphi_{245}/8^{1/2} \\ & & \nu_3 & \varphi_{344}/4 & \varphi_{355}/4 & \varphi_{345}/8^{1/2} \\ & & & 2\nu_4 & 0 & 0 \\ & & & & 2\nu_5 & 0 \\ & & & & & \nu_{4+}\nu_5 \end{vmatrix} \qquad (4)$$

C. Polarization Spectroscopy

The electric field dependence of the band centered at 3113 cm^{-1} (indicated by * in Fig. 4) is measured as the ratio of the field ON to field OFF signal over a range of applied field strengths, and this is shown as the black trace in Fig. 5. This band was selected because it does not significantly overlap with other bands, and we assign this feature to the $C_{(2)}$-H stretch transition of isomer **3**. For isomer **3**, the squares of the eigenvector coefficients for the upper level of this transition are $c^2_{\nu 1}$=0.006, $c^2_{\nu 2}$=0.003, $c^2_{\nu 3}$=0.54, $c^2_{2\nu 4}$=0.18, $c^2_{2\nu 5}$=0.037, and $c^2_{\nu 4+\nu 5}$=0.23, indicating the substantial mode mixing described above. The field ON:OFF intensity ratio is simulated by assuming the *ab initio* μ_p for isomer **3** (10.8 D), and this simulation is shown as the red squares in Fig. 5. Also shown are the simulations for three hypothetical structures having dipole moments equal to 5, 9 and 15 D. For all four simulations, the VTMA (α) is set to 37º, which is chosen to reproduce the asymptotic (high-field limit) field dependence. We note that because the 3113 cm^{-1} band is a member of an anharmonic resonance polyad, the experimentally derived VTMA (37º) *cannot* in general be compared to the *ab initio* VTMA obtained from the harmonic frequency computation (≈27 º for the $C_{(2)}$-H stretch of isomer **3**), and the VTMA here serves only as a single adjustable fitting parameter. In the limit of infinite field, the asymptotic field dependence is due only to the VTMA (α), and is independent of μ_p (as long

as μ_p is finite). For example, when α=0º, 54.75º or 90º (parallel polarization) the high field limit of the ON:OFF intensity ratios are 3, 1, or 0, respectively. However, the rate at which these asymptotic limits are approached depends strongly on the *magnitude* of μ_p. Indeed, the μ_p=5 D system approaches more slowly the asymptotic limit than that with a μ_p equal to 9 D. Clearly, there is excellent agreement between the experimental trace and the simulation that assumes an isomer **3** structure and permanent dipole moment. From this polarization spectroscopy measurement, we assign a dipole moment of 11±2 D to the carrier of this IR band. Again, this agrees quite well with the predicted μ_p for isomer **3**, and more generally, it agrees with the range of dipole moments (9-13 D) that are predicted for all [emim$^+$][Tf_2N^-] ion-pair isomers. The computed magnitudes of μ_p for isomers **1**-**5** are 9.9, 9.7, 10.8, 10.7 and 11.0, respectively. Indeed, this result provides rather definitive confirmation that ion-pairs are the main constituents of [emim$^+$][Tf_2N^-] vapor at 420 K.

Previous VUV photoionization studies of [emim$^+$][Br^-] showed that vaporization occurs via the evolution of alkyl bromides and alkylimidazoles, rather than the intact ion-pairs.[86] Experimental activation enthalpies were found to be in good agreement with computations of the formation of these species, in which the ion-pair thermal decomposition pathway consists of an S_N2 reaction involving the bromide anion and either of the alkyl substituents on the IM ring.[86] The decomposition of [emim$^+$][Tf_2N^-] via this mechanism would produce methylimidazole or ethylimidazole, which have computed dipole moments of 4.2 and 4.3 D, respectively. Another feasible decomposition pathway is proton transfer from [emim$^+$] to [Tf_2N^-] to produce 1-ethyl-3-methylimidazole 2-carbene (2.4 D dipole moment).[87, 88] In general, decomposition products are expected to have dipole moments that are qualitatively smaller than those computed for the intact ion-pair. The polarization spectroscopy reported here indicates that these decomposition pathways for [emim$^+$][Tf_2N^-] are negligible at 420 K, and its vaporization at this temperature largely produces intact ion-pairs.

Conclusions

The ionic liquid 1-ethyl-3-methylimidazolium bis(trifluoromethylsulfonyl)imide was vaporized at 420 K, solvated in 0.4 K He nanodroplets and probed with IR laser spectroscopy. The experimental conditions were such that each He droplet picked up a single molecule from the gas phase. The IR spectrum in the CH stretch region was measured, and it reveals bands that are assigned to intact $[emim^+][Tf_2N^-]$ ion-pairs. The assignment is based on a comparison of the IR spectrum to *ab initio* harmonic frequency computations of 23 ion-pair isomers that were found to be local minima at the MP2/aug-cc-pVTZ level of theory.

The agreement between the experimental and computed IR spectra is improved by taking into account the anharmonic coupling between the IM CH stretch fundamentals and the overtones and combination of two IM ring stretching vibrations near 1600 cm^{-1}. For isomers having a strong H-bond between the cation and anion, the H-bonded donor $C_{(2)}H$ stretch on the IM ring is shifted to lower energy and into resonance with the ring stretching overtones and combination. The anharmonic coupling between these modes results in a resonance polyad consisting of four peaks centered near 3075 cm^{-1} that are spread over ≈100 cm^{-1}. The experimental IR spectrum agrees qualitatively with this characteristic four peak pattern predicted for the H-bonded ion-pair isomers. This pattern of transitions is absent for isomers lacking a strong, directional $C_{(2)}H^{+\cdots}$anion H-bond, and the $C_{(2)}H$ stretching band in these "stacked" isomers are predicted as single transitions in the 3125-3175 cm^{-1} range. Vibrational bands are observed in this wavelength range, indicating that non-H-bonded, stacked isomers are also present in the ensemble of droplets. The experimental IR spectrum is therefore consistent with the pick-up and cooling of ion-pairs by He droplets, in which the cooling is sufficiently fast to freeze out the thermal distribution of the vapor (at 420 K).

The assignment to intact $[emim^+][Tf_2N^-]$ ion-pairs is confirmed with polarization spectroscopy, in which the permanent electric dipole moment of the He-solvated species is oriented in a lab-frame dc electric field. The electric field dependence of several IR band intensities is consistent with a He-solvated molecule that has a dipole moment in the range 11±2 D. The computed magnitudes of μ_p for $[emim^+][Tf_2N^-]$ ion-pair isomers are indeed between 9 and 13 D, and the lowest free energy isomer computed at the MP2/aug-cc-pVTZ level has a 10.8

D dipole moment. The potential products of thermal decomposition have computed dipole moments that are considerably lower (<4.3 D) than those found for the intact ion-pairs. The polarization spectroscopy employed here therefore indicates that the thermal decomposition of [$emim^+$][Tf_2N^-] is negligible at 420 K, and that its vaporization at this temperature largely produces intact ion-pairs.

The results presented here are inconsistent with previous interpretations of the IR spectra of liquid [$emim^+$][Tf_2N^-], in which the temperature, pressure and dilution effects on the hydrogen bonding network in the liquid were analyzed in terms of the number and relative intensities of bands in the IM CH stretch region, without consideration of anharmonic polyads.[46] As originally suggested by Lassègues and co-workers,[53] anharmonic resonances in the CH stretch region cannot be neglected in these analyses. However, contrary to previous suggestions,[53] H-bonding interactions in the liquid are also essential to explain the complexity in the 3050-3150 cm^{-1} region of the condensed phase IR spectra, as discussed by Ludwig and co-workers.[50] Indeed, this is now particularly evident from the spectra of the cold, He nanodroplet isolated species, in which both H-bonding interactions and anharmonic coupling to overtones and combination states must be invoked to rationalize the spectra.

Acknowledgments

G.E.D acknowledges generous support from the National Science Foundation (CHE-1054742). This work was supported in part by a grant of computer time from the Department of Defense High Performance Computing Modernization Program at the Air Force Research Laboratory DoD Supercomputing Resource Center. S.D.C. gratefully acknowledges funding from the U.S. Air Force Office of Scientific Research (Grant No. FA9300-06-C-0023).

References

1. *Ionic Liquids in Synthesis*. Wiley-VCH: Weinheim, Germany, 2003.

2. Castner, E. W.; Wishart, J. F. Spotlight on Ionic Liquids. *J. Chem. Phys.* **2010,** *132*, 120901.

3. Passerini, S.; Shin, J. H.; Henderson, W. A. Peo-Based Polymer Electrolytes with Ionic Liquids and Their Use in Lithium Metal-Polymer Electrolyte Batteries. *J. Electrochem. Soc.* **2005,** *152*, A978-A983.

4. Henderson, W. A.; Shin, J. H.; Passerini, S. Ionic Liquids to the Rescue? Overcoming the Ionic Conductivity Limitations of Polymer Electrolytes. *Electrochem. Commun.* **2003,** *5*, 1016-1020.

5. Chen, L. Q.; Hu, Y. S.; Li, H.; Huang, X. J. Novel Room Temperature Molten Salt Electrolyte Based on Litfsi and Acetamide for Lithium Batteries. *Electrochem. Commun.* **2004,** *6*, 28-32.

6. Wang, P.; Zakeeruddin, S. M.; Moser, J. E.; Gratzel, M. A New Ionic Liquid Electrolyte Enhances the Conversion Efficiency of Dye-Sensitized Solar Cells. *J. Phys. Chem. B* **2003,** *107*, 13280-13285.

7. Zakeeruddin, S. M.; Wang, P.; Wenger, B.; Humphry-Baker, R.; Moser, J. E.; Teuscher, J.; Kantlehner, W.; Mezger, J.; Stoyanov, E. V.; Gratzel, M. Charge Separation and Efficient Light Energy Conversion in Sensitized Mesoscopic Solar Cells Based on Binary Ionic Liquids. *J. Am. Chem. Soc.* **2005,** *127*, 6850-6856.

8. Watanabe, M.; Susan, M. A. B. H.; Noda, A.; Mitsushima, S. Bronsted Acid-Base Ionic Liquids and Their Use as New Materials for Anhydrous Proton Conductors. *Chem. Commun.* **2003**, 938-939.

9. de Souza, R. F.; Padilha, J. C.; Goncalves, R. S.; Dupont, J. Room Temperature Dialkylimidazolium Ionic Liquid-Based Fuel Cells. *Electrochem. Commun.* **2003,** *5*, 728-731.

10. Blanchard, L. A.; Hancu, D.; Beckman, E. J.; Brennecke, J. F. Green Processing Using Ionic Liquids and CO_2. *Nature* **1999,** *399*, 28-29.

11. Plechkova, N. V.; Seddon, K. R. Applications of Ionic Liquids in the Chemical Industry. *Chem. Soc. Rev.* **2008,** *37*, 123-150.

12. Larriba, C.; Castro, S.; de la Mora, J. F.; Lozano, P. Monoenergetic Source of Kilodalton Ions from Taylor Cones of Ionic Liquids. *J. Appl. Phys.* **2007,** *101,* 084303.

13. Lozano, P. C. Energy Properties of an EMI-Im Ionic Liquid Ion Source. *J. Phys. D Appl. Phys.* **2006,** *39,* 126-134.

14. Chiu, Y. H.; Dressler, R. A., Ionic Liquids for Space Propulsion. In *Ionic Liquids IV: Not Just Solvents Anymore* Brennecke, J. F.; Rogers, R. D.; Seddon, K. R., Eds. American Chemical Society: Washington, DC, 2007; Vol. 231, p 138.

15. Chambreau, S. D.; Schneider, S.; Rosander, M.; Hawkins, T.; Gallegos, C. J.; Pastewait, M. F.; Vaghjiani, G. L. Fourier Transform Infrared Studies in Hypergolic Ignition of Ionic Liquids. *J. Phys. Chem. A* **2008,** *112,* 7816-7824.

16. Schneider, S.; Hawkins, T.; Rosander, M.; Vaghjiani, G.; Chambreau, S.; Drake, G. Ionic Liquids as Hypergolic Fuels. *Energ. Fuel* **2008,** *22,* 2871-2872.

17. Zhang, Y.; Shreeve, J. M. Dicyanoborate-Based Ionic Liquids as Hypergolic Fluids. *Angew. Chem. Int. Edit.* **2011,** *50,* 935-937.

18. Zhang, Y.; Gao, H.; Guo, Y.; Joo, Y.-H.; Shreeve, J. M. Hypergolic N,N-Dimethylhydrazinium Ionic Liquids. *Chem. Eur. J.* **2010,** *16,* 3114-3120.

19. He, L.; Tao, G.-H.; Parrish, D. A.; Shreeve, J. M. Nitrocyanamide-Based Ionic Liquids and Their Portential Applications as Hypergolic Fuels. *Chem. Eur. J.* **2010,** *16,* 5736-5743.

20. Schneider, S.; Hawkins, T.; Rosander, M.; Mills, J.; Vaghjiani, G.; Chambreau, S. Liquid Azide Salts and Their Reactions with Common Oxidizers Irfna and N_2O_4. *Inorg. Chem.* **2008,** *47,* 6082-6089.

21. Schneider, S.; Hawkins, T.; Ahmed, Y.; Rosander, M.; Hudgens, L.; Mills, J. Green Bipropellants: Hydrogen-Rich Ionic Liquids That Are Hypergolic with Hydrogen Peroxide. *Angew. Chem. Int. Edit.* **2011,** *50,* 5886-5888.

22. Earle, M. J.; Esperanca, J. M. S. S.; Gilea, M. A.; Lopes, J. N. C.; Rebelo, L. P. N.; Magee, J. W.; Seddon, K. R.; Widegren, J. A. The Distillation and Volatility of Ionic Liquids. *Nature* **2006,** *439,* 831-834.

23. Armstrong, J. P.; Hurst, C.; Jones, R. G.; Licence, P.; Lovelock, K. R. J.; Satterley, C. J.; Villar-Garcia, I. J. Vapourisation of Ionic Liquids. *Phys. Chem. Chem. Phys.* **2007,** *9,* 982-990.

24. Strasser, D.; Goulay, F.; Belau, L.; Kostko, O.; Koh, C.; Chambreau, S. D.; Vaghjiani, G. L.; Ahmed, M.; Leone, S. R. Tunable Wavelength Soft Photoionization of Ionic Liquid Vapors. *J. Phys. Chem. A* **2010,** *114*, 879-883.

25. Koh, C. J.; Liu, C. L.; Harmon, C. W.; Strasser, D.; Golan, A.; Kostko, O.; Chambreau, S. D.; Vaghjiani, G. L.; Leone, S. R. Soft Ionization of Thermally Evaporated Hypergolic Ionic Liquid Aerosols. *J. Phys. Chem. A* **2011,** *115*, 4630-4635.

26. da Piedade, M. E. M.; Leal, J. P.; Esperanca, J. M. S. S.; Lopes, J. N. C.; Rebelo, L. P. N.; Seddon, K. R. The Nature of Ionic Liquids in the Gas Phase. *J. Phys. Chem. A* **2007,** *111*, 6176-6182.

27. Chambreau, S. D.; Boatz, J. A.; Vaghjiani, G. L.; Friedman, J. F.; Eyet, N.; Viggiano, A. A. Reactions of Ions with Ionic Liquid Vapors by Selected-Ion Flow Tube Mass Spectrometry. *J. Phys. Chem. Lett.* **2011,** *2*, 874-879.

28. Maginn, E. J.; Kelkar, M. S. Calculating the Enthalpy of Vaporization for Ionic Liquid Clusters. *J. Phys. Chem. B* **2007,** *111*, 9424-9427.

29. Strasser, D.; Goulay, F.; Kelkar, M. S.; Maginn, E. J.; Leone, S. R. Photoelectron Spectrum of Isolated Ion-Pairs in Ionic Liquid Vapor. *J. Phys. Chem. A* **2007,** *111*, 3191-3195.

30. Zaitsau, D. H.; Kabo, G. J.; Strechan, A. A.; Paulechka, Y. U.; Tschersich, A.; Verevkin, S. P.; Heintz, A. Experimental Vapor Pressures of 1-Alkyl-3-Methylimidazolium Bis(Trifluoromethylsulfonyl) Imides and a Correlation Scheme for Estimation of Vaporization Enthalpies of Ionic Liquids. *J. Phys. Chem. A* **2006,** *110*, 7303-7306.

31. Chambreau, S. D.; Vaghjiani, G. L.; To, A.; Koh, C.; Strasser, D.; Kostko, O.; Leone, S. R. Heats of Vaporization of Room Temperature Ionic Liquids by Tunable Vacuum Ultraviolet Photoionization. *J. Phys. Chem. B* **2010,** *114*, 1361-1367.

32. Koh, C. J.; Leone, S. R. Simultaneous Ion-Pair Photodissociation and Dissociative Ionization of an Ionic Liquid: Velocity Map Imaging of Vacuum-Ultraviolet-Excited 1-Ethyl-3-Methylimidazolium Bis(Trifluoromethylsulfonyl)Imide. *Mol. Phys.* **2012,** *110*, 1705-1712.

33. Gross, J. H. Molecular Ions of Ionic Liquids in the Gas Phase. *J. Am. Soc. Mass Spectr.* **2008,** *19*, 1347-1352.

34. Chambreau, S. D.; Vaghjiani, G. L.; Koh, C. J.; Golan, A.; Leone, S. R. Ultraviolet Photoionization Efficiency of the Vaporized Ionic Liquid 1-Butyl-3-Methylimidazolium

Tricyanomethanide: Direct Detection of the Intact Ion Pair. *J. Phys. Chem. Lett.* **2012,** *3*, 2910-2914.

35. Carper, W. R.; Meng, Z.; Dolle, A. Gas Phase Model of an Ionic Liquid: Semi-Empirical and Ab Initio Bonding and Molecular Structure. *J. Mol. Struc-Theochem* **2002,** *585*, 119-128.

36. Liu, K. H.; Pu, M.; Chen, B. H. DFT Study on the Structure of Ionic Liquid 1-Ethyl-3-Methylimidazolium Hexafluorophosphate. *Chinese J. Struc. Chem.* **2005,** *24*, 576-580.

37. Liu, K. H.; Pu, M.; Li, H. Y.; Chen, B. H. Quantum Chemistry Study of the Ionic Liquid 1-Ethyl-3-Methylimidazolium Tetrafluoroborate. *Chinese J. Chem. Phys.* **2005,** *18*, 331-335.

38. Hunt, P. A.; Gould, I. R. Structural Characterization of the 1-Butyl-3-Methylimidazolium Chloride Ion Pair Using ab initio Methods. *J. Phys. Chem. A* **2006,** *110*, 2269-2282.

39. Palomar, J.; Ferro, V. R.; Gilarranz, M. A.; Rodriguez, J. J. Computational Approach to Nuclear Magnetic Resonance in 1-Alkyl-3-Methylimidazolium Ionic Liquids. *J. Phys. Chem. B* **2007,** *111*, 168-180.

40. Hunt, P. A. Why Does a Reduction in Hydrogen Bonding Lead to an Increase in Viscosity for the 1-Butyl-2,3-Dimethyl-Imidazolium-Based Ionic Liquids? *J. Phys. Chem. B* **2007,** *111*, 4844-4853.

41. Kirchner, B.; Lehmann, S. B. C.; Roatsch, M.; Schoppke, M. On the Physical Origin of the Cation-Anion Intermediate Bond in Ionic Liquids Part I. Placing a (Weak) Hydrogen Bond between Two Charges. *Phys. Chem. Chem. Phys.* **2010,** *12*, 7473-7486.

42. Tsuzuki, S.; Tokuda, H.; Hayamizu, K.; Watanabe, M. Magnitude and Directionality of Interaction in Ion Pairs of Ionic Liquids: Relationship with Ionic Conductivity. *J. Phys. Chem. B* **2005,** *109*, 16474-16481.

43. Tsuzuki, S.; Tokuda, H.; Mikami, M. Theoretical Analysis of the Hydrogen Bond of Imidazolium C-2-H with Anions. *Phys. Chem. Chem. Phys.* **2007,** *9*, 4780-4784.

44. Akai, N.; Parazs, D.; Kawai, A.; Shibuya, K. Cryogenic Neon Matrix-Isolation FTIR Spectroscopy of Evaporated Ionic Liquids: Geometrical Structure of Cation-Anion 1:1 Pair in the Gas Phase. *J. Phys. Chem. B* **2009,** *113*, 4756-4762.

45. Weingärtner, H. Understanding Ionic Liquids at the Molecular Level: Facts, Problems, and Controversies. *Angew. Chem. Int. Edit.* **2008,** *47*, 654-670.

46. Koddermann, T.; Wertz, C.; Heintz, A.; Ludwig, R. Ion-Pair Formation in the Ionic Liquid 1-Ethyl-3-Methylimidazolium Bis(Triflyl)Imide as a Function of Temperature and Concentration. *Chemphyschem* **2006,** *7*, 1944-1949.

47. Jeon, Y.; Sung, J.; Seo, C.; Lim, H.; Cheong, H.; Kang, M.; Moon, B.; Ouchi, Y.; Kim, D. Structures of Ionic Liquids with Different Anions Studied by Infrared Vibration Spectroscopy. *J. Phys. Chem. B* **2008,** *112*, 4735-4740.

48. Hofft, O.; Bahr, S.; Kempter, V. Investigations with Infrared Spectroscopy on Films of the Ionic Liquid [Emim]Tf2N. *Langmuir* **2008,** *24*, 11562-11566.

49. Hofft, O.; Bahr, S.; Kempter, V. Rairs Investigations on Films of the Ionic Liquid [Emim]Tf2N. *Anal. Sci.* **2008,** *24*, 1273-1277.

50. Roth, C.; Chatzipapadopoulos, S.; Kerle, D.; Friedriszik, F.; Lutgens, M.; Lochbrunner, S.; Kuhn, O.; Ludwig, R. Hydrogen Bonding in Ionic Liquids Probed by Linear and Nonlinear Vibrational Spectroscopy. *New J. Phys.* **2012,** *14*, 105026.

51. Akai, N.; Kawai, A.; Shibuya, K. First Observation of the Matrix-Isolated Ftir Spectrum of Vaporized Ionic Liquid: An Example of Emimtfsi, 1-Ethyl-3-Methylimidazolium Bis(Trifluoromethanesulfonyl)Imide. *Chem. Lett.* **2008,** *37*, 256-257.

52. Akai, N.; Kawai, A.; Shibuya, K. Ion-Pair Structure of Vaporized Ionic Liquid Studied by Matrix-Isolation Ftir Spectroscopy with Dft Calculations: A Case of 1-Ethyl-3-Methylimidazolium Trifluoromethanesulfonate. *J. Phys. Chem. A* **2010,** *114*, 12662-12666.

53. Lassegues, J. C.; Grondin, J.; Cavagnat, D.; Johansson, P. New Interpretation of the CH Stretching Vibrations in Imidazolium-Based Ionic Liquids. *J. Phys. Chem. A* **2009,** *113*, 6419-6421.

54. Grondin, J.; Lassegues, J. C.; Cavagnat, D.; Buffeteau, T.; Johansson, P.; Holomb, R. Revisited Vibrational Assignments of Imidazolium-Based Ionic Liquids. *J. Raman Spectrosc.* **2011,** *42*, 733-743.

55. Wulf, A.; Fumino, K.; Ludwig, R. Comment on "New Interpretation of the CH Stretching Vibrations in Imidazolium-Based Ionic Liquids". *J. Phys. Chem. A* **2010,** *114*, 685-686.

56. Lassegues, J. C.; Grondin, J.; Cavagnat, D.; Johansson, P. Reply to the "Comment on 'New Interpretation of the CH Stretching Vibrations in Imidazolium-Based Ionic Liquids'". *J. Phys. Chem. A* **2010,** *114*, 687-688.

57. Choi, M. Y.; Douberly, G. E.; Falconer, T. M.; Lewis, W. K.; Lindsay, C. M.; Merritt, J. M.; Stiles, P. L.; Miller, R. E. Infrared Spectroscopy of Helium Nanodroplets: Novel Methods for Physics and Chemistry. *Int. Rev. Phys. Chem.* **2006,** *25*, 15-75.

58. Toennies, J. P.; Vilesov, A. F. Superfluid Helium Droplets: A Uniquely Cold Nanomatrix for Molecules and Molecular Complexes. *Angew. Chem. Int. Edit.* **2004,** *43*, 2622-2648.

59. Toennies, J. P.; Vilesov, A. F.; Whaley, K. B. Superfluid Helium Droplets: An Ultracold Nanolaboratory. *Physics Today* **2001,** *54*, 31-37.

60. Toennies, J. P.; Vilesov, A. F. Spectroscopy of Atoms and Molecules in Liquid Helium. *Annu. Rev. Phys. Chem.* **1998,** *49*, 1-41.

61. Lehmann, K. K.; Scoles, G. Superfluid Helium - the Ultimate Spectroscopic Matrix? *Science* **1998,** *279*, 2065-2066.

62. Stienkemeier, F.; Lehmann, K. K. Spectroscopy and Dynamics in Helium Nanodroplets. *J. Phys. B-At. Mol. Opt.* **2006,** *39*, R127-R166.

63. Choi, M. Y.; Dong, F.; Miller, R. E. Multiple Tautomers of Cytosine Identified and Characterized by Infrared Laser Spectroscopy in Helium Nanodroplets: Probing Structure Using Vibrational Transition Moment Angles. *Philos. T. R. Soc. A* **2005,** *363*, 393-412.

64. Choi, M. Y.; Miller, R. E. Four Tautomers of Isolated Guanine from Infrared Laser Spectroscopy in Helium Nanodroplets. *J. Am. Chem. Soc.* **2006,** *128*, 7320-7328.

65. Lewerenz, M.; Schilling, B.; Toennies, J. P. A New Scattering Deflection Method for Determining and Selecting the Sizes of Large Liquid Clusters of He-4. *Chem. Phys. Lett.* **1993,** *206*, 381-387.

66. Knuth, E. L.; Schilling, B.; Toennies, J. P., In *International Symposium on Rarefied Gas Dynamics*, Harvey, J.; Lord, G., Eds. Oxford University Press: Oxford, UK, 1995; Vol. 19, pp 270-276.

67. Hartmann, M.; Miller, R. E.; Toennies, J. P.; Vilesov, A. Rotationally Resolved Spectroscopy of SF_6 in Liquid-Helium Clusters - a Molecular Probe of Cluster Temperature. *Phys. Rev. Lett.* **1995,** *75*, 1566-1569.

68. Hartmann, M.; Miller, R. E.; Toennies, J. P.; Vilesov, A. F. High-Resolution Molecular Spectroscopy of Van Der Waals Clusters in Liquid Helium Droplets. *Science* **1996,** *272*, 1631-1634.

69. Brink, D. M.; Stringari, S. Density of States and Evaporation Rate of Helium Clusters. *Z. Phys. D-Atom Mol. Cl.* **1990,** *15*, 257-263.

70. Morrison, A. M.; Liang, T.; Douberly, G. E. Automation of an "Aculight" Continuous-Wave Optical Parametric Oscillator. *Rev. Sci. Instrum.* **2013,** *84*, 013102.

71. Pople, J. A.; Binkley, J. S.; Seeger, R. Theoretical Models Incorporating Electron Correlation. *Int. J. Quantum Chem.* **1976**, 1-19.

72. Frisch, M. J.; Head-Gordon, M.; Pople, J. A. A Direct MP2 Gradient-Method. *Chem. Phys. Lett.* **1990,** *166*, 275-280.

73. Aikens, C. M.; Webb, S. P.; Bell, R. L.; Fletcher, G. D.; Schmidt, M. W.; Gordon, M. S. A Derivation of the Frozen-Orbital Unrestricted Open-Shell and Restricted Closed-Shell Second-Order Perturbation Theory Analytic Gradient Expressions. *Theor. Chem. Acc.* **2003,** *110*, 233-253.

74. Dunning, T. H. Gaussian-Basis Sets for Use in Correlated Molecular Calculations .1. The Atoms Boron through Neon and Hydrogen. *J. Chem. Phys.* **1989,** *90*, 1007-1023.

75. Dunning, T. H.; Peterson, K. A.; Wilson, A. K. Gaussian Basis Sets for Use in Correlated Molecular Calculations. X. The Atoms Aluminum through Argon Revisited. *J. Chem. Phys.* **2001,** *114*, 9244-9253.

76. Schmidt, M. W.; Baldridge, K. K.; Boatz, J. A.; Elbert, S. T.; Gordon, M. S.; Jensen, J. H.; Koseki, S.; Matsunaga, N.; Nguyen, K. A.; Su, S. J.; Windus, T. L.; Dupuis, M.; Montgomery, J. A. General Atomic and Molecular Electronic-Structure System. *J. Comput. Chem.* **1993,** *14*, 1347-1363.

77. Gordon, M. S.; Schmidt, M. W., Theory and Applications of Computational Chemistry, the First Forty Years. Dykstra, C. E.; Frenking, G.; Kim, K. S., Eds. Elsevier: Amsterdam, 2005; pp 1167-1189.

78. Dong, F.; Miller, R. E. Vibrational Transition Moment Angles in Isolated Biomolecules: A Structural Tool. *Science* **2002,** *298*, 1227-1230.

79. Douberly, G. E.; Miller, R. E. The Growth of HF Polymers in Helium Nanodroplets: Probing the Barriers to Ring Insertion. *J. Phys. Chem. B* **2003,** *107*, 4500-4507.

80. Kong, W.; Bulthuis, J. Orientation of Asymmetric Top Molecules in a Uniform Electric Field: Calculations for Species without Symmetry Axes. *J. Phys. Chem. A* **2000,** *104*, 1055-1063.

81. Kong, W.; Pei, L. S.; Zhang, J. Linear Dichroism Spectroscopy of Gas Phase Biological Molecules Embedded in Superfluid Helium Droplets. *Int. Rev. Phys. Chem.* **2009,** *28,* 33-52.

82. Franks, K. J.; Li, H. Z.; Kong, W. Orientation of Pyrimidine in the Gas Phase Using a Strong Electric Field: Spectroscopy and Relaxation Dynamics. *J. Chem. Phys.* **1999,** *110,* 11779-11788.

83. Buchenau, H.; Toennies, J. P.; Northby, J. A. Excitation and Ionization of He-4 Clusters by Electrons. *J. Chem. Phys.* **1991,** *95,* 8134-8148.

84. Nielsen, H. H. The Vibration-Rotation Energies of Molecules. *Rev. Mod. Phys.* **1951,** *23,* 90-136.

85. Hoy, A. R.; Mills, I. M.; Strey, G. Anharmonic Force Constant Calculations. *Mol. Phys.* **1972,** *24,* 1265-1290.

86. Chambreau, S. D.; Boatz, J. A.; Vaghjiani, G. L.; Koh, C.; Kostko, O.; Golan, A.; Leone, S. R. Thermal Decomposition Mechanism of 1-Ethyl-3-Methylimidazolium Bromide Ionic Liquid. *J. Phys. Chem. A* **2012,** *116,* 5867-5876.

87. Holloczki, O.; Gerhard, D.; Massone, K.; Szarvas, L.; Nemeth, B.; Veszpremi, T.; Nyulaszi, L. Carbenes in Ionic Liquids. *New J. Chem.* **2010,** *34,* 3004-3009.

88. Rodriguez, H.; Gurau, G.; Holbrey, J. D.; Rogers, R. D. Reaction of Elemental Chalcogens with Imidazolium Acetates to Yield Imidazole-2-Chalcogenones: Direct Evidence for Ionic Liquids as Proto-Carbenes. *Chem. Commun.* **2011,** *47,* 3222-3224.

Figure Captions

Figure 1: Five low energy [$emim^+$][Tf_2N^-] ion-pair structures (electronic +ZPVE) at the MP2/aug-cc-pVTZ level of theory.

Figure 2: a) Mass spectrum of the He droplet beam with the [$emim^+$][Tf_2N^-] source off. Peaks at multiples of 4 u are due to He_n^+ cluster ions. The peak at m/z=18 u is due to a small fraction of the droplets (<1%) that have picked up residual water molecules in the vacuum chamber. The mass spectrum of the droplet beam with the [$emim^+$][Tf_2N^-] source heated to b) 408 K, c) 418 K, and d) 426 K shows the gradual appearance of the intact [$emim^+$] cation at m/z=111 u. Temperatures are obtained with a K-type thermocouple attached to the quartz furnace.

Figure 3: The mass spectrum of the neat droplet beam was scaled and subtracted from the mass spectrum with 426 K oven temperature conditions in order to reduce contributions from the He_n^+ peaks. In addition to the [$emim^+$] peak at m/z=111 u, peaks at 31, 50, 64, and 69 u are observed and are due to CF^+, CF_2^+, SO_2^+, and CF_3^+, which are fragments from [Tf_2N^-]. Peaks at m/z=27, 28, and 29 u are characteristic fragment peaks of [$emim^+$] associated with the ethyl side chain.

Figure 4: Helium Droplet IR spectrum in the CH stretch region for [$emim^+$][Tf_2N^-] vapor. The He droplet spectrum corresponds to the wavelength dependent ion signal depletion in the m/z=111 u channel. The top (red) simulated spectrum is a Boltzmann weighted sum of the computed harmonic frequency spectra (scaled by 0.96) for the five lowest free energy isomers computed at the MP2/aug-cc-pVTZ level. The bottom (blue) simulated spectrum is a Boltzmann weighted sum of the computed anharmonic frequency spectra for these same five isomers. The peaks marked by # are the four transitions associated with the anharmonic resonance polyad that involves the H-bonded $C_{(2)}$-H stretch and the IM ring stretching overtones and combination.

Figure 5: Field ON:OFF intensity ratio for the 3113 cm^{-1} band as a function of the applied orientation field. The laser polarization is aligned parallel to the static field, and the asymptotic dependence of the signal indicates a VTMA close to ≈37 degrees. The smooth lines are simulations of the field dependence for several different magnitudes of the permanent electric dipole moment, as given in the inset. The rate at which the signal approaches the asymptotic limit is consistent with a permanent electric dipole moment of 11±2 D.

Figure 1

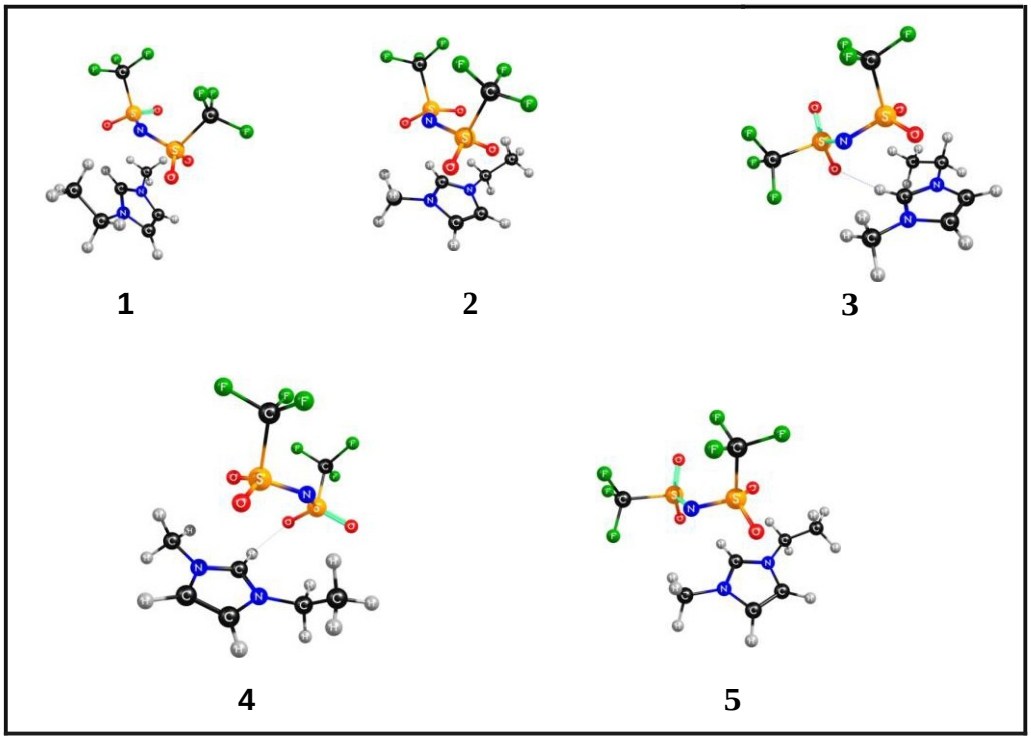

Figure 2

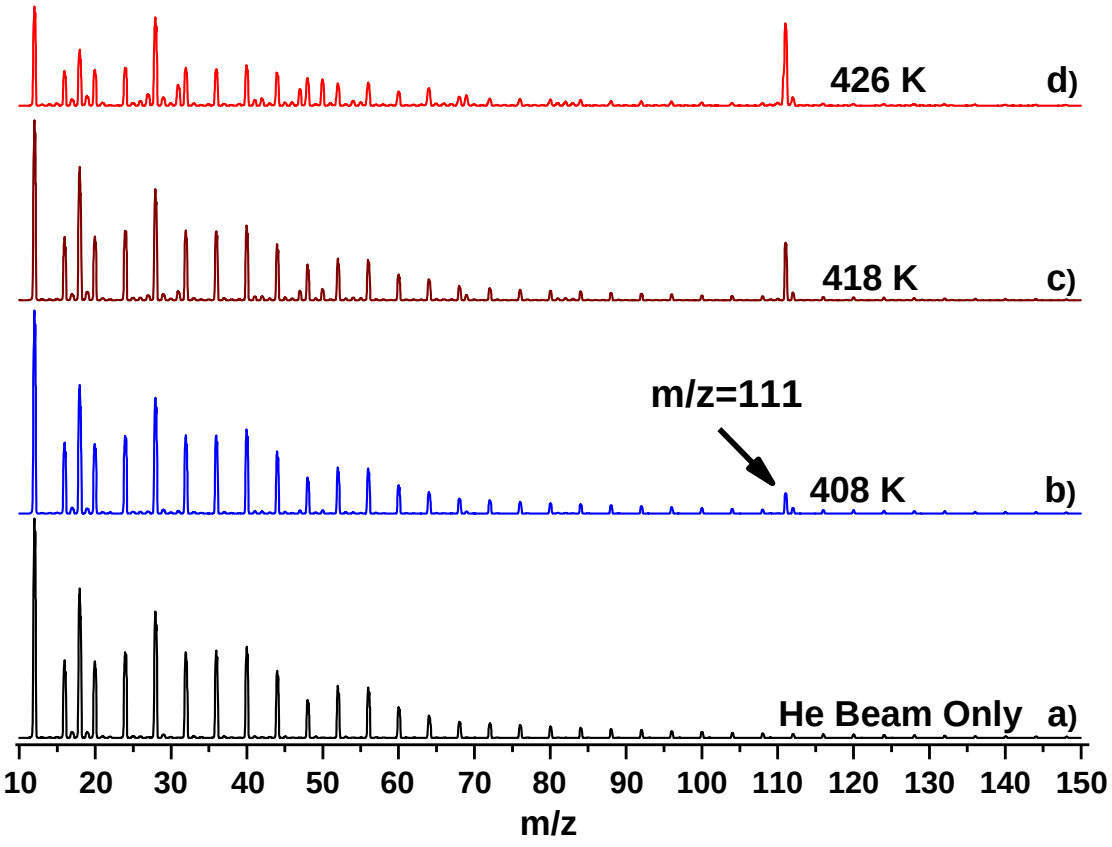

Figure 3

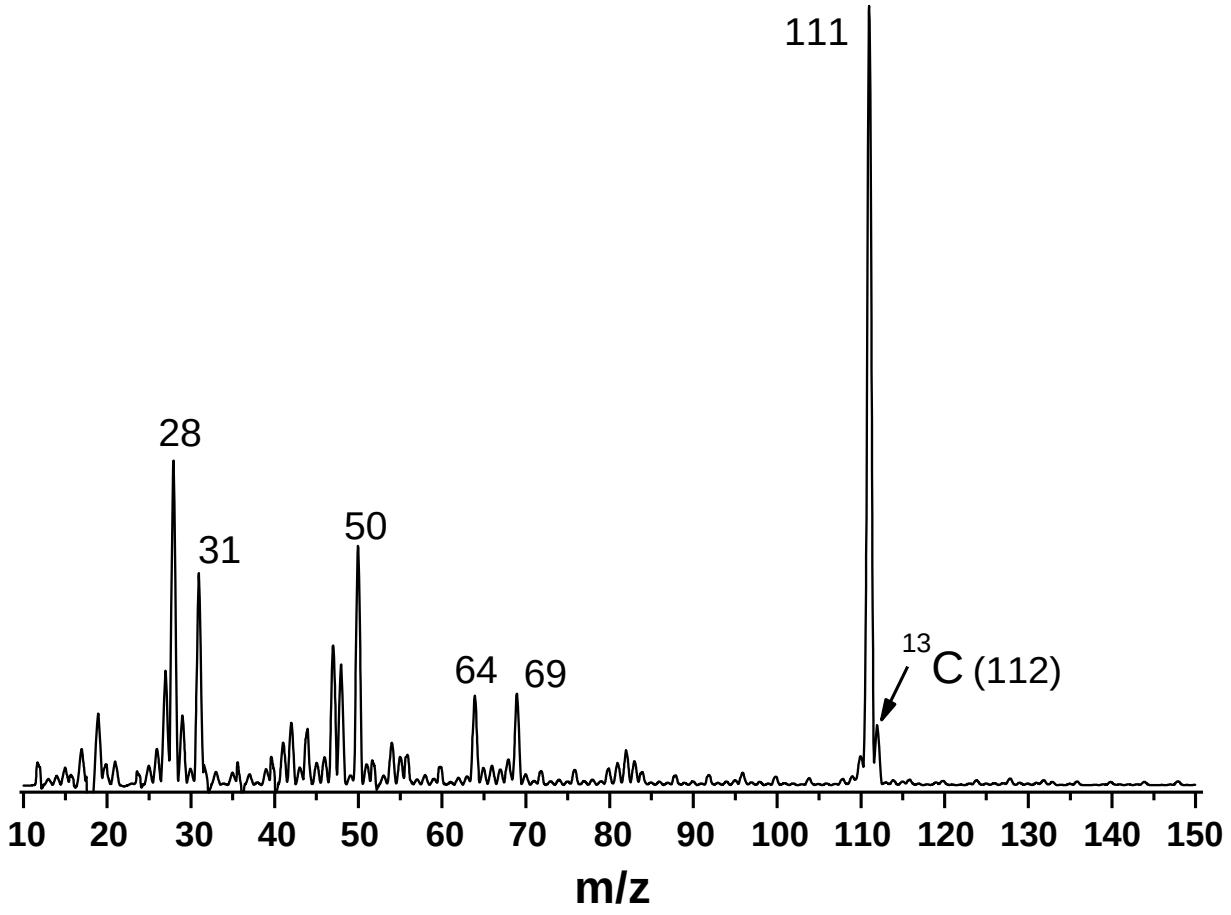

Figure 4

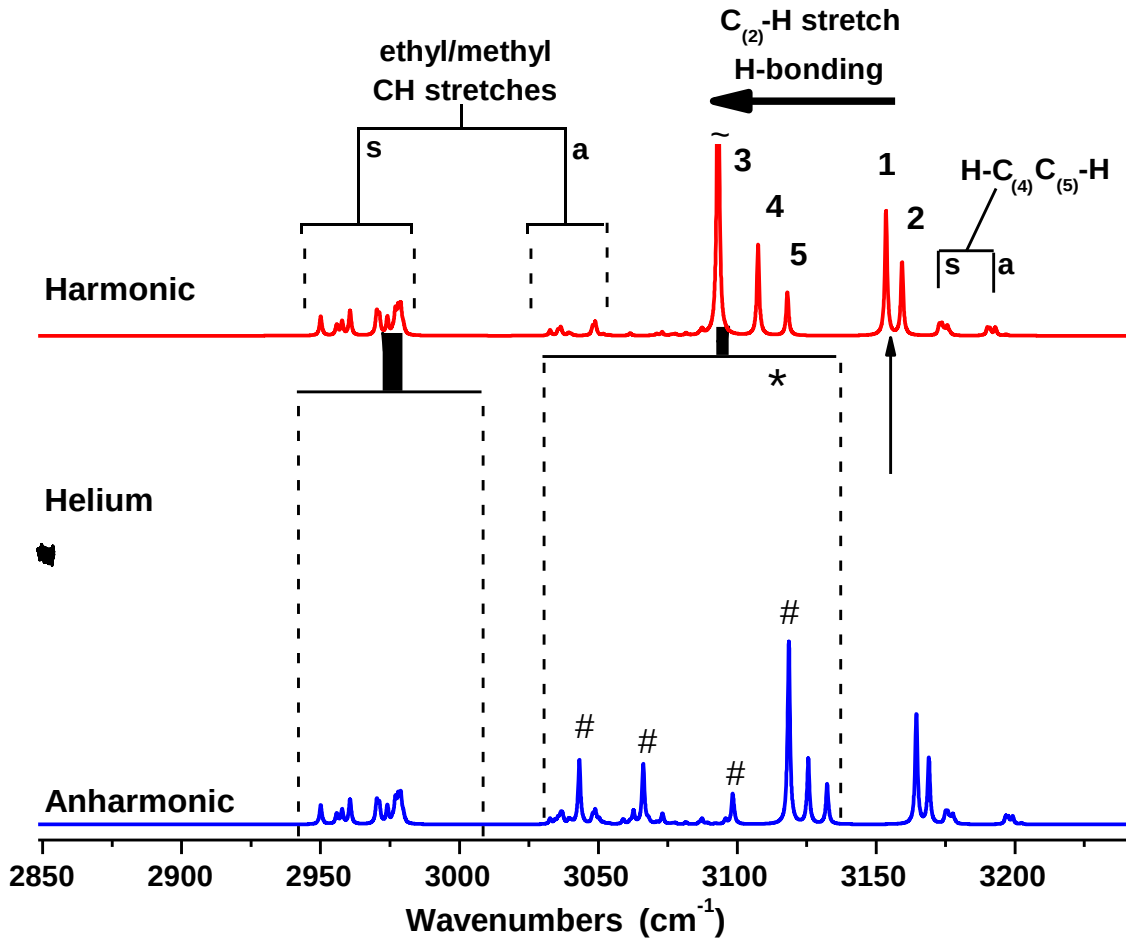

Figure 5